Analysis of Simulated and Experimental Fluorescence Recovery After Photobleaching. Data for Two Diffusing Components

Gerald W. Gordon, Brad Chazotte, Xue Feng Wang, and Brian Herman
Laboratories for Cell Biology, Department of Cell Biology and Anatomy, University of North Carolina at Chapel Hill, Chapel Hill, North Carolina 27599-7090 USA

ABSTRACT Fluorescence recovery after photobleaching has been a popular technique to quantify the lateral mobility of membrane components. A variety of analysis methods have been used to determine the lateral diffusional mobility, *D*. However, many of these methods suffer from the drawbacks that they are not able to discern two-component diffusion (i.e., three-point fit), cannot solve for two components (linearization procedures), and do not perform well at low signal-to-noise. To overcome these limitations, we have adopted the approach of fitting fluorescence recovery after photobleaching curves by the full series solution using a Marquardt algorithm. Using simulated data of one or two diffusing components, determinations of the accuracy and reliability of the method with regard to extraction of diffusion parameters and the differentiation of one- versus two-component recovery curves were made under a variety of conditions comparable with those found in actual experimental situations. The performance of the method was also examined in experiments on artificial liposomes and fibroblast membranes labeled with fluorescent lipid and/or protein components. Our results indicate that: 1) the method was capable of extracting one- and two-component *D* values over a large range of conditions; 2) the *D* of a one-component recovery can be measured to within 10% with a small signal (100 prebleach photon counts per channel); 3) a two-component recovery requires more than 100-fold greater signal level than a one-component recovery for the same error; and 4) for two-component fits, multiple recovery curves may be needed to provide adequate signal to achieve the desired level of confidence in the fitted parameters and in the differentiation of one- and two-component diffusion.

INTRODUCTION

Fluorescence recovery after photobleaching (FRAP) has proved to be a popular means to assess the structure of artificial and biological membranes. It is based on the principal of observing the rate of recovery of fluorescence due to the movement of a fluorescent marker into an area of the membrane that contains this same marker but that has been rendered nonfluorescent via an intense photobleaching pulse of laser light (e.g., Elson, 1985; Kapitza and Jacobson, 1986; Peters, 1986; Wolf, 1989). The two-dimensional diffusion coefficient (D) of the fluorophore is related to both its rate and extent of recovery. A number of procedures have been developed to extract D from fluorescence recovery curves. Axelrod et al. (1976) have developed two spot photobleaching analysis procedures that could be applied to both Gaussian and uniform circular laser beam profiles. The first relies on the use of a simple, three-point fitting procedure that is dependent on knowing the initial fluorescence, the fluorescence immediately after bleaching, the maximum recovered fluorescence, and the nature of the lateral transport (diffusion or flow). From these measured values, the half-time of recovery can be determined, and thus D. The second, a more sophisticated graphical curve fitting procedure, involves overlaying experimental curves on theoretical curves to get a good shape match and, although the method is tolerant of incomplete recovery, it seems cumbersome and slow and sensitive to noise.

Fitting the FRAP data to a linearized approximation of the theoretical recovery curve has been used by a number of authors (Petersen et al., 1986; Elson and Qian, 1989; Soumpasis, 1983; Barisas and Leuther, 1983; van Zoelen et al., 1983; Yguerabide et al., 1982). Linearization approaches have the advantage that two diffusing components can be detected, but the measurement of recovery parameters for two components is not possible. The relative merits of many of these approaches has been reviewed by Petersen et al. (1986). A more recent adaptation that measures recovery parameters for two diffusing components and that is more accurate for shallow bleaches than deep bleaches has been published by Greenberg and Axelrod (1993).

The prime motivation for development of the method described in this paper was the need to analyze two-component recovery curves in the presence of significant noise due to low signal levels. (Throughout this paper, a one-component recovery is defined as resulting from one diffusing component and its immobile fraction, and a two-component recovery is defined as resulting from two diffusing components and their respective immobile fractions.) Typical FRAP studies of cells membranes show significant photon counting noise in the individual data points, which is the limiting factor in analysis of FRAP data collected at a low signal level. Noise prevents accurate determination of the recovery parameters such as D and makes discrimination between one and two diffusing components difficult. We therefore adopted a method of high accuracy but with low sensitivity

Received for publication 19 May 1994 and in final form 25 October 1994.
Address reprint requests to Department of Cell Biology & Anatomy, The University of North Carolina at Chapel Hill, CB #7090, 232 Taylor Hall, Chapel Hill, NC 27599-7090. Tel.: 919-966-5507; Fax: 919-966-1856; E-mail: bhfg@med.unc.edu.
© 1995 by the Biophysical Society
0006-3495/95/03/766/13 $2.00

to noise. The method is derived from that of Petersen et al. (1986), which uses several terms in a series closely approximating the theoretical recovery curve, which is a gamma function. The method exploited the fact that noise results principally from photon counting and is Poisson-distributed. The effect of smoothing the recovery curve as applied by Petersen et al. (1986) and our method's ability to accurately extract two-component data from artificial planar lipid bilayers or cells labeled with fluorescent phospholipids and/or protein were also determined. In the simulations, the error (based on the SD) of estimations of the recovery parameters (e.g., D) was determined by the Monte Carlo method instead of the less reliable asymptotic standard error method (Bevington, 1969). These parameter errors were then used to quantify the effects of changing experimental conditions (e.g., beam diameter, dwell time, signal level, depth of bleach), to optimize conditions through minimization of the error measurement. After the one- and two-component fits were done on each recovery curve, an F-test was used to distinguish one- and two-component systems. Our results indicate that the method can distinguish one- and two-component data reliably. Two-component fits required more than 100-fold larger signal levels than one-component fits to get the same parameter errors and, thus, optimization of the instrumental parameters such as dwell time and beam diameter is critical for the success of the two-component fit. In both cell and artificial membranes, the method was able to determine recovery parameters with a high degree of accuracy given that the number of diffusing components is known.

MATERIALS AND METHODS

Liposome preparation

Cell-sized liposomes were prepared according to the methods of Mueller et al. (1983) as described in Florine-Casteel et al. (1990). 25 mg of 1,2,-dioeyl-*sn*-glycerol-3-phosphatidyl choline in 1.0 ml of chloroform (Avanti Polar Lipids, Alabaster, AL) was mixed with 3,3′-dioctadecylindocarbocyanine (DiI), a fluorescent lipid analog, in ethanol at a ratio of 5000:1. The mixture was evaporated to dryness in an Erlenmeyer flask under argon gas and 100 ml of deoxygenated, distilled, deionized water was subsequently added. The hydrated mixture was allowed to remain at 4°C in the dark for 48 h to permit vesicle formation. Vesicles were harvested by Pasteur pipette and placed on a covered microscope slide with paper shims for FRAP measurements (Chazotte et al., 1985).

Cell preparation

Mouse fibroblast 3T3 cells were cultured, plated on glass microscope coverslips, and mounted for FRAP measurements as described previously (Jacobson et al., 1984). Cells were labeled as follows. For integral membrane protein diffusion, rhodamine-labeled anti-GP80 IgG was added to cells as described previously (Jacobson et al., 1984). For membrane lipid diffusion, 1 mg/ml stock solution of Rhodamine-PE (Molecular Probes, OR) in ethanol was added to the medium, bathing the cells to give a final concentration of 1 μg/ml. The amount added was adjusted to give roughly the same fluorescent intensity as the immunofluorescently labeled cells. When cells were double-labeled for protein and lipid diffusion measurements, the above agents were added to the same cell sample in the same proportions.

FRAP measurements

FRAP measurements were carried out using the instrument detailed in Chazotte and Hackenbrock (1988). The 514-nm line from the Argon ion laser was used as the excitation source. A variety of different Leitz lenses were used: 25× 0.5 NA, 40× 0.7 NA, 40× 1.3 NA oil, and a 100× 1.3 NA oil. Different dwell times were selected as required, and signal averaging was used for some samples where appropriate, e.g., liposomes. All measurements were carried out at 21°C.

Curve-fitting software

To analyze experimental FRAP data, two computer programs were developed, an analysis program for experimental data and a simulation program to evaluate the performance of the analysis program. The analysis program used experimental data as input and the fitted parameters and goodness of fit statistics as output. The experimental data include user defined locations (in channel numbers) of the prebleach, recovery, and baseline (dark noise) portions of the experiment. The simulation program used an input file describing the simulation to be performed and wrote fitted parameters with error estimates and goodness of fit statistics to an output file. Both programs used the same fitting algorithm, which uses the Marquardt method as presented in Bevington (1969). The Marquardt method is an example of nonlinear, least-squared error fitting and is therefore an iterative method. The starting point for algorithm and software development was a one-diffusing component, FRAP curve-fitting program kindly provided to us by Dr. N. O. Petersen. In this program, the data were smoothed to reduce processing time (by reducing the number of points in the recovery curve presented to the fitting algorithm). Petersen et al. (1986) found smoothing improved their estimates of τ.

The current versions of the programs were developed on a SparcStation using the Gnu C compiler, gcc (Free Software Foundation, Cambridge, MA) and then recompiled for MS-DOS machines (80386 and up microprocessors with math coprocessor) using the djgpp C compiler, which is gcc ported to MS-DOS by D. J. Delorie (internet electronic mail to djgpp@sun.soe.clarkson.edu). Both of these compilers are free and are available from Austin Code Works (Austin, TX) and via anonymous ftp from various sites. The use of gcc allows the same source code to be used under both MS-DOS and SunOS and has the further advantage of using the faster native 80386 instructions instead of the 8086 instructions of normal MS-DOS programs. The time for curve fit analysis (including both one- and two-component fits) of a simulated recovery curve was about 1 min on a 25-MHz 80386 computer that housed an 80387 math coprocessor. Poisson noise used in the simulations was generated using algorithms described in the book "Numerical Recipes in C" (Press et al. 1988) and required some modification to prevent run-time range and domain errors. The quality of the random noise was verified by determination of the mean and variance of the Poisson noise generator.

Five significant changes were made to the curve-fitting procedure compared with that described by Peterson (1986). 1) The current model value was used as the estimate of the variance for each point in the calculation of the weighted sum of squared errors. This gave better results than using the data point value itself as the estimate of its own variance. The rationale for this change was that when the data have significant noise, the model value approaches the true value (the mean value) of that data point and is therefore a better approximation to the variance of the distribution of possible values of the data point than is the data point itself. 2) Smoothing the recovery curve was made an option. Although the smoothed curve is faster to fit, the time to fit without smoothing was reasonable, and the results were better. 3) The parameters were constrained never to take values normally considered to be physically impossible (e.g., negative characteristic times and mobile fractions outside the range of 0.0–1.0 inclusive). This was done after noticing that many poor results and failures to fit involved impossible parameter values such as negative mobile fractions. Essentially all simulation results were usable with this modification. 4) The ability to perform a two-component fit in which both components have the same depth of bleach. This models an experiment where one species of fluorescent probe is used to label two different, independently diffusing membrane components.

5) The ability to analyze recovery curves collected in the "pulse mode," which is an intermittent form of data collection using a shutter that is opened periodically to limit exposure of the specimen to the monitoring beam.

FRAP model

For the one-component recovery curve, we follow Axelrod et al. (1976) and Petersen et al. (1986). Let F_i be the prebleach intensity, $F(0)$ be the first postbleach intensity, and K be the solution of

$$F(0) = F_i[1 - \exp(-K)]/K. \quad (1)$$

K is a measure of the fractional depth of bleach, $F(0)/F_i$. The one-component model takes the form

$$F(t) = \phi F_i f(t) + (1 - \phi)F(0), \quad (2)$$

where $F(t)$ is the intensity at time t, ϕ is the mobile fraction, and $f(t)$ is the series

$$f(t) = \sum_{n=0}^{\infty} \left[\frac{(-K)^{-n}}{n!}\right]\left(1 + n + \frac{2nt}{\tau}\right)^{-1}, \quad (3)$$

where τ is the characteristic time of diffusion. To form the two-component model, two one-component recovery curves are added together. The subscripts 1 and 2 distinguish the two diffusing components with a common K value. The model is based on the two series

$$f_1(t) = \sum_{n=0}^{\infty} \left[\frac{(-K)^{-n}}{n!}\right]\left(1 + n + \frac{2nt}{\tau_1}\right)^{-1} \quad (4)$$

and

$$f_2(t) = \sum_{n=0}^{\infty} \left[\frac{(-K)^{-n}}{n!}\right]\left(1 + n + \frac{2nt}{\tau_2}\right)^{-1}. \quad (5)$$

The two-component model then becomes

$$F(t) = \alpha[\phi_1 F_i f_1(t) + (1 - \phi_1) F(0)] + (1 - \alpha)[\phi_2 F_i f_2(t) + (1 - \phi_2)F(0)], \quad (6)$$

where α is the fraction of component 1. This model has six parameters, K, τ_1, τ_2, α, ϕ_1, and ϕ_2. However, three of the parameters, α, ϕ_1, and ϕ_2, are dependent, meaning that their values cannot be determined uniquely. Even though the six-parameter model works well, the five-parameter model below performs better at lower signal levels and, thus, the five-parameter model was used to produce the results in the present report. Substituting Eq. 1 for $F(0)$ in Eq. 6 and rearranging yields

$$F(t) = F_i\{\alpha\phi_1 f_1(t) + (1 - \alpha)\phi_2 f_2(t) + [1 - (\alpha\phi_1 + (1 - \alpha)\phi_2)][(1 - \exp(-K))/K]\}. \quad (7)$$

In Equation 7 the three parameters α, ϕ_1, and ϕ_2 occur only as the products $\alpha\phi_1$ and $(1 - \alpha)\phi_2$, indicating that they are dependent. The two products are used in place of the three original parameters, which yields two independent parameters ($\alpha\phi_1$ and $(1 - \alpha)\phi_2$) for a total of five parameters. The two products are the mobile fractions weighted by the component fractions (weighted mobile fractions) and are represented as w_1 and w_2 in the tables. Thus, it is not possible to determine uniquely either the mobile fractions or the component fraction, but only the weighted mobile fractions. The fraction of the fluorescence due to immobile molecules of both components (net or aggregate immobile fraction), before the bleach is $1 - (\alpha\phi_1 + (1 - \alpha)\phi_2)$.

Analysis algorithm

The first step in the analysis is a three-point fit (Axelrod et al., 1976) that estimates the half-time of recovery, the depth of bleach parameter (K), and the mobile fraction (ϕ) assuming one diffusing component. The three-point fit method measures three intensity values relative to the baseline (dark noise): the prebleach intensity, the intensity immediately after the bleach, and the intensity at the last part of the recovery curve, which is assumed to be at complete recovery (Axelrod et al., 1976). Smoothing of the recovery curve is then performed if desired. A smoothed point is created by taking a contiguous group of points in the raw recovery curve and replacing the group with a single point usually derived by averaging the group or interpolating within the group. The smoothing algorithm used is that of Petersen et al. (1986) and is adaptive in that it starts with one raw data point to a group for the first postbleach point and increases the group size by two after every two groups. This samples the early, fast rising part of the curve best and smooths the late, slow rising part the most. The three-point fit estimates are used as the starting guesses for a one-component fit, which assumes the one-component model above (Eq. 2). The results of the one-component fit are recorded and also used to generate starting guesses for the two-component fit, which assumes the two-component model above (Eq. 7). For both models the number of terms of the series (Eq. 3 for the one-component model or Eqs. 4 and 5 for the two-component model) increased with the estimated value of K as in Petersen et al. (1986). The number of points of the recovery curve to be analyzed may be varied by the user, but was typically 976. The results of the analysis program are the fitted parameters, the reduced χ^2 values for the one- and two-component fits, and the F-test values comparing the two fits.

Simulation program

The inputs to the simulation program are the true parameters (using the six parameters of Eq. 6) of the simulated experimental photobleach and recovery data, the mean background intensity, the dwell time (which is the acquisition channel duration), the number of times to repeat each experiment, and a set of prebleach intensities that form a family of experiments that differ only in signal-to-noise ratio. The mobile fractions and component fractions are used to specify the simulation because they represent the underlying physical system even though the two-component fit can determine only the weighted mobile fractions. Another input is a seed for the random number generator. The true parameters are used to generate a noiseless data set that is scaled to the first prebleach intensity. Fig. 1 illustrates noiseless, one-component recovery curves for the range of D values used in the simulations. Poisson noise is then added to produce a data set to analyze. Fig. 2 illustrates a two-component recovery curve with noise plus the fitted curve superimposed. Each data set analyzed has a different pattern of Poisson noise. The curve-fitting proceeds as in the analysis program with the addition that the results of all the repetitions of one prebleach intensity are collected to produce a Monte Carlo estimate of the means and variances of the fitted parameters. After all repetitions of a single prebleach intensity, the

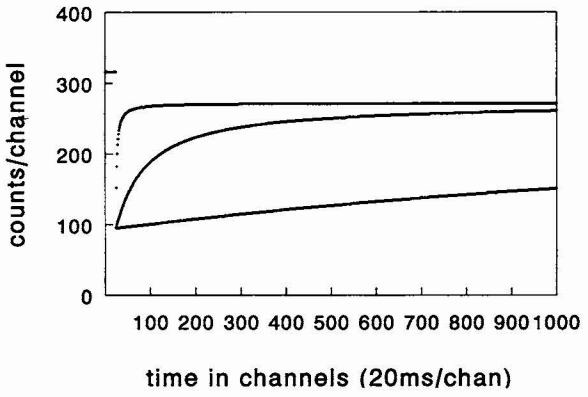

FIGURE 1 Three noiseless, simulated recovery curves visually representing the range of diffusion coefficients considered. The one diffusing component diffusion coefficient for the top one is 1e-7 cm^2/s, the middle is 3e-9 cm^2/s, and the bottom is 1e-10 cm^2/s. All have 316 prebleach counts per channel, 70% bleach depth, 80% mobile fraction, and 20-ms dwell time for 976 channels of recovery.

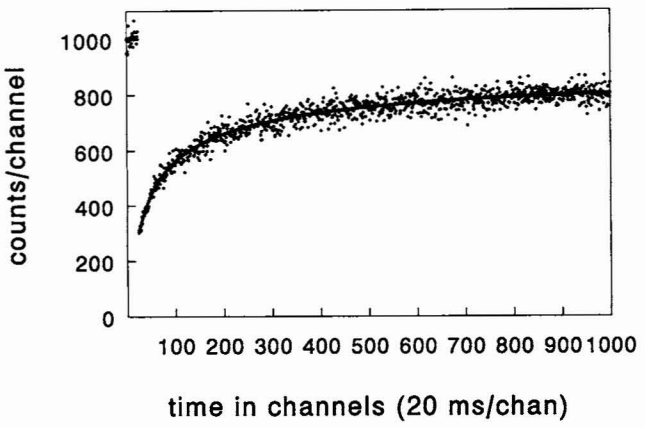

FIGURE 2 A simulated, two-component recovery curve with noise. The two diffusion coefficients are $1e-9$ and $5e-9$ cm^2/s, and the fraction of the slow component is 0.5. The mean prebleach counts per channel is 1000, both bleach depths are 70%, both mobile fractions are 80%, and the dwell time is 20 ms for 976 channels of recovery.

noiseless data are scaled to a new prebleach intensity and the process is repeated. Each input file is given a unique seed for the random number generator to ensure a negligible chance of repeating a pattern of Poisson noise.

All simulations had 976 data points (channels) in the recovery curve and no dark current (zero baseline). Many of the simulations had the standard values of beam diameter 2.24 micrometers, fractional depth of bleach 0.7, mobile fraction 0.8, fraction of the slower diffusing component 0.5, and dwell time of 20 ms. No simulations were smoothed, and all simulations used 50 terms of the series (Eq. 3 or Eqs. 4 and 5) used to generate the noiseless curve. Each set of input parameter values was used to generate 32 recovery curves that were fitted and the results tabulated and summarized. The number of repetitions (32) was chosen because 20 samples are enough to estimate the mean and variance of a Gaussian distribution (Hoel et al., 1971), and 32 repetitions could be expected to produce at least 20 samples even if some trials failed.

Two types of information were used in evaluating the results, the fraction of cases in which one- and two-component fits could be correctly identified and the means and coefficients of variation of the parameter values. The coefficient of variation (c.v.) is defined as the SD divided by the true value of the parameter. In the SD calculation, the sum of the squared differences between the fitted value and the true value was used. Thus, a c.v. of 0.5 indicates a SD of about half the value of the parameter. The c.v. was chosen for comparison because the raw parameter values varied widely and the normalized quality of the c.v. facilitated comparisons. By using the true value as the reference point (instead of the sample mean), both the error in the sample mean and the variation in the estimated parameter contribute to the c.v., allowing the quality of the estimate to be characterized by a single number. In calculating the mean and c.v., only fits with χ^2 values significant at the 5% level were included.

It was possible for a fit to fail to produce a result due to, for example, a failure to converge or a math error such as division by zero. The failure rate on simulated data is quite small because of the constraints imposed on the parameters during the iterative fitting. In 29,600 data sets fitted for this study, there were 4 failures and all occurred in doing two-component fits of one-component data.

In discriminating between one- and two-component data, no fits were excluded on the basis of χ^2 values. If both one- and two-component fits failed, the data were excluded. If one fit failed, the other was accepted by default. If both fits succeeded, the χ^2 values were compared using an F-test to determine which fit to accept. For the F-test, the significance level of the decrease in the χ^2 value due to addition of the second diffusing component was determined.

RESULTS

Three-point fit

The three-point fit method of Axelrod et al. (1976) was used to generate initial estimates of the various parameter values for the one-component curve fit method. The three-point-fit method generates an estimate of the half-time of recovery. To convert the estimate of the half-time of recovery to an estimate of the characteristic time of recovery (τ) from which D (the diffusion coefficient in cm^2/s) can be calculated, a correction factor based on the depth of bleach (Axelrod et al., 1976) had to be applied. The accuracy of the three-point-fit method in estimating values of D over three orders of magnitude was determined, and the mean values of 32 fits of each D are summarized in Table 1. All of the simulations in Table 1 have mobile fraction (ϕ) equal to 0.8, a fractional depth of bleach equal to 0.7 (corresponding to $K = 3.2$), a dwell time (acquisition channel duration) of 20 ms and a prebleach signal level of 100 photon counts per channel. Over of the range of D reported in Table 1, four of the seven mean estimates of D were within a factor of two of the true value, and six were within a factor of 3.3, a reasonable degree of accuracy. At small D values, the mean estimate of ϕ is very low because the recovery of fluorescence is not sampled long enough and, therefore, the last data points recorded are significantly below the value they would take at infinite time. At large D values, the mean estimate of K is very low because the first data point during the early, fast rising part of the recovery curve is the average over an interval of time (the dwell time) during which there is a significant increase in fluorescence intensity and, therefore, the fluorescence intensity at the beginning of the recovery curve is overestimated. Correction factors based on the ratio of the estimated τ and the dwell time could be applied to improve the mean estimates of ϕ and K, but this approach was not pursued because the curve-fitting procedures described below provided more accurate data than expected from a corrected three-point fit. Increasing the signal resulted in at best small

TABLE 1 Accuracy of the three-point fit method as a function of *D*

True D	1.00e-10	3.00e-10	1.00e-09	3.00e-09	1.00e-08	3.00e-08	1.00e-07
Cnts/chan	100	100	100	100	100	100	100
D mean	1.47e-09	9.89e-10	1.68e-09	3.79e-09	9.98e-09	2.31e-08	4.61e-08
ϕ mean	0.24	0.47	0.66	0.75	0.77	0.77	0.69
K mean	3.17	3.24	3.05	3.08	2.92	2.44	1.53

Each column shows the results for the D in the top row. The true mobile fraction was 0.8, the true depth of bleach 0.7 ($K = 3.2$), and dwell time of 20 ms.

TABLE 2 Accuracy of three-point fit as a function of signal level

Cnts/chan	100	316	1000	3162	10,000	True
D mean	3.79e-09	3.65e-09	3.41e-09	3.33e-09	3.30e-09	3.00e-09
ϕ mean	0.75	0.75	0.75	0.74	0.75	0.80
K mean	3.08	3.16	3.08	3.09	3.10	3.20

Each column shows results for a different signal level as indicated in the cnts/chan row. The true values are the same for each signal level and are shown in the last column. The dwell time is 20 ms for all.

improvement in the mean of D and no improvement in the means of the other two parameters for any given D using the three-point-fit method (Table 2). This somewhat surprising result may mean that the intrinsic errors of the three-point-fit method are greater than the error due to noise even at the lowest signal level used.

One-diffusing-component curve fit

Using the same recovery curves as for the three-point fit, it was found that the means of the various parameters examined were superior and less dependent on the ratio of τ to the dwell time when the curve fit approach was used (Table 3). The mean D values were all within 20% of the true values, and four of seven were within 3%. If the two extreme values of D are excluded, the results were excellent. At the smallest D, the c.v. of K is small and the uncertainty in ϕ is the likely cause of the uncertainty in D. At the largest D, the c.v. of K is large and is the likely cause of the uncertainty in D. The rejection of the two-component model was very reliable in that the two-component fit was never accepted over the one-component fit. The fraction of cases in which the two-component fit was accepted over the one-component fit is indicated in the row labeled "frac acc 2" of Table 3. The row labeled "n valid" contains the number of trials out of 32 in which the one-component fit had a χ^2 significant at the 5% level. The lowest c.v. occurs for $D = 3 \times 10^{-9}$ cm^2/s, corresponding to a ratio of τ to dwell time of 52.3. Near this optimum value of the ratio, the c.v. did not change rapidly and, for values of the ratio differing by a factor of 3.16 (the square root of 10), the c.v.s were nearly indistinguishable from those at the optimum ratio value (Table 3).

The effect of signal level on the accuracy of one-component curve-fitting for determination of D with the smallest c.v. from Table 3 was examined, and the data are reported in Table 4. The last column has the true values of the parameters, which are the input values to the simulation and the values that would be recovered by curve fitting given a noiseless signal. The decrease in the c.v. for D was found to be less than a factor of two for a factor of 3.16 increase in signal level. The rejection of a two-component model remained very reliable as the signal level increased. In any situation with noise, there is a finite probability that the program will find a minimum in the error surface that is not acceptably close to the true parameters. The one case in which the two-component model was accepted ("frac acc 2" = 0.03 or 1 out of 32) appears to be such an occurrence.

The basic parameter values used in the simulations (300 counts per channel prebleach signal, dwell time at 20 ms, and 0.7 depth of bleach) are representative of values found in actual FRAP measurements; therefore, excellent results would be expected from fitting experimental data resulting from a specimen with one diffusing component using the curve-fitting procedure described in this study.

The dwell time and beam diameter were altered in an attempt to improve the curve fit (Tables 5–7). For the smallest diffusion coefficient (1×10^{-10} cm^2/s), increasing the dwell time (with no change in the monitoring beam power) increased the quality of the fit (Table 5). Increasing the dwell time resulted in both the ratio of τ to dwell time becoming closer to the optimum ratio (as determined from Table 3) as well as the signal level increasing. The increase in dwell time caused a sevenfold decrease in the c.v. of D as compared with a factor of less than two, which would be predicted from increasing the signal level alone (Table 4). Increasing the dwell time in this way increases the amount of bleaching by the monitoring beam during one measurement, so care must be exercised to ensure that the extent of the bleaching is kept insignificant to maintain the validity of the results.

TABLE 3 One-component fit of one-component data

True D	1.00e-10	3.00e-10	1.00e-09	3.00e-09	1.00e-08	3.00e-08	1.00e-07
Cnts/chan	100	100	100	100	100	100	100
Frac acc 2	0.00	0.00	0.00	0.00	0.00	0.00	0.00
n valid	31	31	30	30	30	29	31
D mean	1.20e-10	3.01e-10	9.92e-10	3.00e-09	1.03e-08	2.82e-08	8.56e-08
D c.v.	0.56	0.17	0.11	0.10	0.13	0.23	0.47
ϕ mean	0.78	0.81	0.81	0.80	0.80	0.80	0.77
ϕ c.v.	0.22	0.10	0.04	0.03	0.03	0.05	0.07
K mean	3.21	3.19	3.14	3.15	3.26	2.98	2.98
K c.v.	0.04	0.04	0.06	0.08	0.09	0.21	0.69

Results are shown as a function of D. True D values are in the top row. All simulations have a true mobile fraction 0.8, true depth of bleach of 0.7 (K = 3.2), and a dwell time of 20 ms. The values in the row labeled "frac acc 2" are the fraction of cases in which the two-component fit is accepted over the one-component fit. The values in the "n valid" row are the number of one-component fits that produced χ^2 values acceptable at the 5% level.

TABLE 4 One-component fit of one-component data as a function of signal level

Cnts/chan	100	316	1000	3162	10,000	True
Frac acc 2	0.00	0.03	0.00	0.00	0.00	
n valid	30	30	30	31	29	
D mean	3.00e-09	3.06e-09	2.99e-09	3.01e-09	2.99e-09	3.00e-09
D c.v.	0.10	0.07	0.04	0.02	0.01	
ϕ Mean	0.80	0.80	0.80	0.80	0.80	0.80
ϕ c.v.	0.03	0.02	0.01	0.01	0.004	
K mean	3.15	3.21	3.17	3.20	3.19	3.20
K c.v.	0.08	0.05	0.02	0.01	0.01	

Signal levels are shown in the top row. The true values of the parameters are shown in the last column. The dwell time was 20 ms for all trials.

TABLE 5 Effect of dwell time for a "small" diffusion coefficient for one-component fit of one-component data

Dwell (ms)	20	63	200	632	
Cnts/chan	100	316	1000	3162	True
n valid	32	29	28	32	
D mean	1.20e-10	1.01e-10	9.96e-11	1.00e-10	1.00e-10
D c.v.	0.56	0.08	0.03	0.02	
ϕ mean	0.78	0.80	0.80	0.80	0.80
ϕ c.v.	0.22	0.04	0.01	0.004	
K mean	3.20	3.21	3.19	3.20	3.20
K c.v.	0.04	0.03	0.02	0.01	

The mean prebleach counts per second (not counts per channel) is the same for all dwell times. The true values are shown in the last column

For the largest diffusion coefficient (1×10^{-7} cm^2/s), decreasing the dwell time (with no change in the monitoring beam power) brought the ratio of τ to dwell time closer to optimal (optimal is 52.3), but also resulted in a decrease in signal level (Table 6). The effects of decreasing the dwell time and signal on the quality of fit have a tendency to cancel each other out, but the loss of signal level eventually dominated. However, fitting of the data when the prebleach counts per channel were as low as 10 was still possible. The cases where failures of the curve fitting occurred in the data in Table 6 were not included in the grand total mentioned above because they occurred under conditions of extremely low signal. An improvement in the quality of the curve fitting would be expected if the signal level were kept constant as the dwell time was decreased.

For a large diffusion coefficient, the effect of increasing the beam diameter as a way of increasing the quality of curve fitting was also examined (Table 7). The dwell time was kept constant, and the monitoring beam power was increased to keep the bleaching by the monitoring beam constant. The bleach beam power was also increased to keep the depth of bleach constant. Under these conditions, the quality of the curve fitting increased, and the increase was primarily because τ increased in proportion to the beam area (and therefore the ratio of to dwell time is larger and closer to optimal (52.3)), and the signal level increased in proportion to the area of the beam. The combination of these effects produces a reduction of the c.v. of *D* by more than a factor of two for each increase in the signal level by a factor of 3.16. This is more than would be predicted for the same increase in signal level in the absence of an increase in the beam diameter as shown in Table 4.

Two diffusing component curve fit

The effect of signal level (measured as counts per channel of the prebleach signal) for a two-component fit of two-component data was also examined (Table 8). In these simulations, the ratio of *D* values was equal to 5 such that the two *D* values bracket the optimal from the one-component data (Table 3). As the signal level increases, more accurate estimation of the parameters becomes possible as indicated by

TABLE 6 Effect of dwell time on a "large" diffusion coefficient for one-component fit of one-component data

Dwell (ms)	20	6.3	2	.63	
Cnts/chan	100	32	10	3	True
Frac acc 2	0.00	0.03	0.31	all failed	
n valid	31	32	15		
D mean	8.56e-08	1.20e-07	1.04e-07		1.00e-07
D c.v.	0.47	0.78	0.53		
ϕ mean	0.77	0.81	0.83		0.80
ϕ c.v.	0.07	0.06	0.14		
K mean	2.98	3.83	2.90		3.20
K c.v.	0.69	0.72	0.34		

The mean prebleach counts per second is the same for all dwell times. The true values are shown in the last column. In one case out of thirty-two with 32 cnts/chan, the data were fitted better by the two-component model; in this case, the two diffusion coefficients were within a factor of two of one another.

TABLE 7 Increased beam diameter improves a one-component fit of one-component data of "large" diffusion coefficient

Beam diam. (μ)	2.24	3.98	7.08	12.60	
Cnts/chan	100	316	1000	3162	True
Dwell (ms)	20	20	20	20	
Frac acc 2	0.00	0.03	0.03	0.00	
n valid	31	30	32	28	
D mean	8.56e-08	1.07e-07	9.99e-08	1.00e-07	1.00e-07
D c.v.	0.47	0.20	0.07	0.02	
ϕ mean	0.77	0.80	0.80	0.80	0.80
ϕ c.v.	0.07	0.02	0.01	0.01	
K mean	2.98	3.35	3.21	3.20	3.20
K c.v.	0.69	0.15	0.06	0.02	

TABLE 8 Effect of signal level measured as prebleach counts per channel for a two-component fit of two-component data

Cnts/chan	100	316	1000	3162	10,000	True
Frac acc 2	0.25	0.59	1.00	1.00	1.00	
n valid	32	31	32	32	30	
$D1$ mean	8.41e-10	8.37e-10	8.10e-10	9.80e-10	1.03e-09	1.00e-09
$D1$ c.v.	0.47	0.34	0.28	0.24	0.13	
$D2$ mean	4.72e-09	4.28e-09	4.40e-09	5.32e-09	5.24e-09	5.00e-09
$D2$ c.v.	0.47	0.30	0.25	0.33	0.20	
$w1$ mean	0.31	0.32	0.33	0.39	0.41	0.40
$w1$ c.v.	0.34	0.29	0.24	0.23	0.13	
$w2$ mean	0.50	0.48	0.48	0.41	0.39	0.40
$w2$ c.v.	0.36	0.32	0.26	0.24	0.14	
K mean	3.27	3.15	3.19	3.22	3.20	3.20
K c.v.	0.12	0.06	0.04	0.03	0.01	

The true values of the parameters are shown in the last column. The dwell time is 20 msec.

a decrease in the c.v. and an increase in the fraction of cases in which the one- and two-component fits could be distinguished. If the criteria for a successful fit are to estimate the parameters with a c.v. of less than 0.5 and to distinguish one- and two-component diffusion with near 100% reliability, then a signal of 1000 counts per channel was required under the above conditions. Although one might desire a smaller c.v., 1000 counts per channel is already a large signal under standard experimental conditions. Increasing the counts per channel even further to 10,000 resulted in lower c.v.s of D_1 and D_2, but they were still greater than the c.v. of D for one-component data with only 100 counts per channel (Table 4).

The effect of altering α (the fraction of the slow component) on the quality of the curve fitting using the above criterion for success was also examined. For an α value of either 0.3 or 0.7, at 1000 counts per channel the c.v.s of the D values were still acceptable although larger, and the fraction of fits in which the two component model was accepted was reduced to 0.97 and 0.88, respectively, compared with 1.00 for an α value of 0.5 (Table 8).

The effect of depth of bleach (4 K values) on two-component fitting using the same pair of D values as in Table 8 is presented in Table 9. The c.v.s of the D values decrease with increasing depth of bleach (first four columns), and the deepest bleach (90%) produces acceptable results at 316 counts per channel prebleach. However, a 90% bleach may be problematic when using biological specimens because the energy required to bleach that deeply may result in irreversible damage to living cells. Another potential difficulty is in

TABLE 9 Effect of depth of bleach on two-component fit of two-component data

True K	0.76	1.59	3.20	10.0	
True depth	0.3	0.5	0.7	0.9	
Cnts/chan	316	316	316	316	True
Frac acc 2	0.03	0.19	0.59	1.00	
n valid	30	30	31	30	
$D1$ mean	1.16e-09	1.03e-09	8.37e-10	8.66e-10	1.00e-09
$D1$ c.v.	0.62	0.40	0.34	0.25	
$D2$ mean	3.65e-09	6.26e-09	4.28e-09	4.42e-09	5.00e-09
$D2$ c.v.	0.47	1.28	0.30	0.18	
$w1$ mean	0.29	0.32	0.32	0.34	0.40
$w1$ c.v.	0.39	0.36	0.29	0.21	
$w2$ mean	0.51	0.48	0.48	0.47	0.40
$w2$ c.v.	0.38	0.35	0.32	0.22	
K mean	0.77	1.61	3.15	10.1	
K c.v.	0.09	0.09	0.06	0.10	

The top row shows the true K and the second row the equivalent fractional depth of bleach. Other true parameter values are shown in the last column.

TABLE 10 The effect of the ratio, D2/D1, on two-component fit of two-component data

True $D1$	1.00e-09	1.00e-09	3.00e-10	1.00e-10	1.00e-10	
True $D2$	2.00e-09	5.00e-09	3.00e-09	3.00e-09	1.00e-08	
True $D2/D1$	2	5	10	30	100	
Cnts/chan	316	316	316	316	316	True
Frac acc 2	0.06	0.59	0.97	1.00	1.00	
n valid	28	31	29	27	29	
$D1$ mean	8.05e-10	8.373e-10	2.43e-10	1.75e-10	1.81e-10	
$D1$ c.v.	0.36	0.36	0.40	1.31	1.24	
$D2$ mean	1.96e-09	4.28e-09	2.49e-09	3.25e-09	1.18e-08	
$D2$ c.v.	0.19	0.30	0.25	0.30	0.32	
$w1$ mean	0.29	0.32	0.40	0.35	0.34	0.40
$w1$ c.v.	0.39	0.29	0.16	0.27	0.29	
$w2$ mean	0.52	0.48	0.45	0.39	0.40	0.40
$w2$ c.v.	0.40	0.32	0.17	0.10	0.06	
K mean	3.26	3.15	3.11	3.22	3.30	3.20
K c.v.	0.05	0.06	0.05	0.05	0.08	

The true values of the diffusion coefficients, $D1$ and $D2$, and their ratio values are shown in the top rows. The last column shows true values other than the diffusion coefficients.

keeping the bleach time short enough in order to satisfy the model, which assumes that the bleach time is negligible. Increasing the depth of bleach reveals an earlier, faster region of the recovery curve and, therefore, aids analysis by increasing the usable information about the shape of the recovery curve.

Table 10 shows results for a series of simulations in which the ratio of the diffusion coefficients of the two components was varied from 2 to 100 with constant prebleach counts per channel and constant dwell. As the ratio increases, the reliability of distinguishing two components from one component increases and is 97% when the ratio is 10. The c.v. of the fast component $D(D_2)$ changes little as the ratio increases, and the c.v. of the slow component $D(D_1)$ generally increases. The only ratio in the table at which both D values have c.v.s less than 0.5 and the reliability of accepting the two component fit is near 1.0 is 10.

The effect of increasing the beam diameter on two-component fitting starting with the conditions in the second column of Table 7 (which has 316 counts per channel prebleach) is shown in Table 11. The second column of Table 11 shows the results when the beam diameter is increased by a factor of 1.78 (the fourth root of 10), the bleach beam power is increased by a factor of 3.16 to keep the depth of bleach constant, the monitoring beam power is increased by a factor of 3.16 to keep its bleaching constant (at the original dwell time), and the dwell time is increased by a factor of 3.16 to keep constant the ratios of the τs to the dwell time. The result of these modifications was that bleaching by the monitoring beam increased by a factor of 3.16, the signal level increased by a factor of 10, and the quality of the curve fitting improved to the point that reliable distinction of two-component from one-component data could be made. These results were equivalent to the results obtained by increasing the monitoring beam power (and its associated bleaching) by a factor of 10 (at constant beam diameter), as shown in the last column of Table 11, which is repeated from Table 8. Under these conditions, increasing the beam diameter a small amount produced a large increase in the signal, and significant improvement in the fit with reduced monitoring beam bleaching compared with simply increasing the monitoring beam power.

Given a fixed number of channels acquired, the dwell time determines the total length of time the recovery curve will be sampled and the density of sampling during the recovery. The dwell time should be longer to estimate better the late part of the recovery curve, and the dwell time should be shorter to sample better the fast rising early part of the recovery curve. The optimal dwell time (the dwell time producing the minimum c.v.s for the fitted D values and the maximum reliability of distinguishing two components from one component) was determined for a two-component recovery curve with true D values of 1×10^{-9} and 5×10^{-9} cm^2/s, the same values used in Tables 8, 9, and 11 (data not shown). Tested values of the dwell time were from $\tau_2/52.3$ (12 ms) to $\tau_1/52.3$ (60 ms) inclusive. For one series of experiments, the prebleach counts per channel was kept constant at 316 (the monitoring beam power was changed in

TABLE 11 The effect of beam diameter on two-component fit of two-component data

Beam diam (μ)	2.24	3.98		2.24
Cnts/chan	316	3162	True	3162
Dwell (ms)	20	63		20
Frac acc 2	0.59	1.00		1.00
n valid	31	31		32
$D1$ mean	8.37e-10	1.00e-09	1.00e-09	9.80e-10
$D1$ c.v.	0.34	0.22		0.24
$D2$ mean	4.28e-09	5.29e-09	5.00e-09	5.32e-09
$D2$ c.v.	0.30	0.31		0.33
$w1$ mean	0.32	0.40	0.40	0.39
$w1$ c.v.	0.29	0.20		0.23
$w2$ mean	0.48	0.40	0.40	0.41
$w2$ c.v.	0.32	0.22		0.24
K mean	3.15	3.20	3.20	3.22
K c.v.	0.06	0.02		0.03

The true values are in the third column. The last column is repeated from Table 8 to compare the effect of changing the beam diameter with simply increasing the monitoring beam power.

inverse proportion to the dwell time, resulting in identical bleaching for all dwell times tested), and tests conducted at α values of 0.3, 0.5, and 0.7. For values of 0.3 and 0.5, the optimal dwell was $\tau_2/52.3$ (12 ms), corresponding to the optimal dwell time for a one-component recovery curve with the D value of the fast component. For $\alpha = 0.7$, the optimal dwell time was approximately 20 ms (data not shown). In another series of tests, the dwell time was changed without altering the beam power. Under these conditions, the signal level increased in proportion to the dwell time and the optimal dwell time was longer and when the slow component predominated ($\alpha = 0.7$) the optimal dwell time was the optimal value for the slow component alone (60 ms).

Liposome studies

Single cell-sized lipid vesicles were labeled with DiI to test the accuracy of our simulation results for the case where only one diffusing component was expected. Of 47 total samples studied, 46 were successfully fit; in 37 of these (80%) the one-component model was favored, and in 9 the two-component model was favored. A mean D of 7×10^{-8} cm^2/s and a mobile fraction of 100% were found for DiI in these lipid vesicles. In liposomes consisting of a single lipid membrane component and a single phase (liquid) DiI exhibits primarily the expected one-component diffusion. These samples measured at various dwell times and beam diameters had a wide range of signal levels with a mean of 790 counts per channel with a SD of 1158.

Cell studies

To determine the ability of the curve-fitting models to deal with one- and two-component diffusion in cell membranes, we prepared three identical sets of fibroblast cells for study on the same afternoon using three different labeling protocols. In the first set, lipid diffusion was measured by labeling with only rhodamine-PE. The one-component fitting yielded mean values of $D = 1.2 \times 10^{-8}$ cm^2/s and a mobile fraction of 82% ($n = 17$). In the second set, protein diffusion was measured by labeling with only rhodamine-conjugated anti-GP80 and yielded $D = 5.7 \times 10^{-10}$ cm^2/s with a mobile fraction of 69% ($n = 15$). The third set of cells was double-labeled with both rhodamine PE and rhodamine-conjugated anti-GP80. Two diffusion coefficients were found from the curve-fitting analysis. In cells that were double-labeled, there was a slow component (mean $D = 6.2 \times 10^{-10}$ cm^2/s with a weighted mobile fraction of 0.38) and a fast component (mean $D = 1.3 \times 10^{-8}$ cm^2/s with a weighted mobile fraction of 0.39, $n = 11$). The weighted mobile fractions of the two-component fit are not directly comparable with the mobile fractions of the one-component fits because there is no estimate of the weighting factors. The close values of the two weighted mobile fractions indicate that the mobile fluorescence signals from the two components are close, but no conclusions can be drawn about component fractions or individual mobile fractions from the two-component fit alone. If the mobile fractions from the one-component fits are applied to the two-component fit, α, the fraction of the slow component, is found to be about 0.55. (These samples also provided a wide range of signal levels. The means and SDs of the signal levels in counts per channel for the three sets of samples were: lipid only, 1716 ± 1360; protein only, 190 ± 181; lipid and protein, 618 ± 461.) The results for simultaneous lipid and protein labeling exhibited excellent agreement with those obtained in cells labeled individually with fluorescent lipid or protein probes and indicate that our curve-fitting methods are very competent in extracting the relevant diffusion parameters in a system designed to be a two-component one.

To determine whether the recovery curves were better fit by one or two components, we compared the χ^2 for one-component fits to the χ^2 values of the two-component fits using a F-test of the significance of the reduction in χ^2 due to adding the second component to the model. In cells labeled with just rhodamine anti-GP80, the one-component model was favored in 14 out of 17 cases. In results including studies done on different days, in cells labeled with only rhodamine-PE, 29 out of 51 were fit better by the one-component model, whereas in cells labeled with DiI, 14 of 33 cases were fit better by the one-component model. These latter results could indicate that lipid domains of differing lateral diffusional mobilities exist in the plasma membranes of fibroblasts (see Discussion). However, it is clear from these studies that determination of one- versus two-component diffusion requires a number of recovery curves to be collected.

DISCUSSION

The primary purpose of this study was to determine the ability of our curve-fitting method to calculate one- and two-component diffusion parameters with maximal accuracy and to distinguish accurately the presence of one- versus two-component diffusion in a membrane. Our analysis is based on FRAP models with one or two discrete diffusion coefficients as opposed to several discrete diffusion coefficients or one or more distributed diffusion coefficients. Diffusion in a living cell plasma membrane could be more complex than our chosen models. To distinguish among the various models, the signal-to-noise ratio of the raw data must be sufficiently large. For example, James and Ware (1985) demonstrate that at signal levels commonly used in biological studies, it is impossible to distinguish whether a fluorescence lifetime decay curve that is not adequately fit by a model with one discrete decay time is best fit by a model with two discrete decay times, several discrete decay times, or one or more distributed decay times. Thus, accurate discrimination of the number and types of components in a fluorescence decay curve or, by analogy, a FRAP curve would require collection of data with a very high signal level or some other means of identifying the appropriate number and type of components (and hence the proper model), independent of curve fitting. These investigators' findings appear to be

generally applicable to many situations in which a single discrete component model is inadequate and the data contain noise.

Applying the results of James and Ware's analysis of simulations of exponential decays of fluorescence (James and Ware, 1985) to the analysis of FRAP curves, we conclude that it is impossible at the expected experimental signal levels to use curve fitting to distinguish statistically among models based on two discrete diffusion coefficients, several discrete diffusion coefficients, or one or more distributed diffusions coefficients in the absence of other independent knowledge of the number and types of diffusing components. Thus, when we accept our two-component model over our one-component model, the more general conclusion is that our one-component model does not adequately fit the data and a more complex model is required. In cases in which there is other evidence that there are, in reality, two discrete diffusion coefficients, the results of fitting to our two-component model may be interpreted as two diffusing components. In cases in which no independent evidence exists as to the number and types of diffusing components, we believe that the two-component analysis presented here may still be useful in characterizing the diffusional components in a membrane. The values resulting from the fit provide significant information about diffusion in the membrane even if the model used has not been demonstrated to be optimal. It is possible that an optimal model could be found by collecting enough FRAP curves under conditions as nearly identical as possible and fitting all the curves together with global analysis. Using the results for fluorescence lifetime measurements (James and Ware, 1985) as a very rough estimate for FRAP analysis, 1582 FRAP curves at the common signal level for integral membrane proteins of 316 counts in the peak channel would be required to provide the 500,000 counts in the peak channel needed to distinguish among the models.

The curve-fitting methods developed in this study fit both one- and two-component data over a wide range of conditions. The use of simulated as well as experimental data permitted definition of the performance limits of the fitting algorithm and provided information of how various instrumental parameters used in FRAP data collection affect the success of the curve fitting and, thus, how best to optimize FRAP data collection. In particular, we examined the success of the curve fitting under conditions of low level fluorescence signal, a condition that is likely to be encountered in studies of the lateral mobilities of integral proteins in cell membranes.

Analysis of one-component diffusion

The fitting of data to the one-component diffusion model was quite robust and rapid. Analyses of simulated data indicated that the one-component model accurately fit D values over three orders of magnitude acquired with the same dwell time and at low signal levels. Curve fitting, which uses all the acquired recovery data, was found, not surprisingly, to be superior to the three-point fit method in determination of recovery curve parameter means and c.v.s and, in particular, had a less stringent requirement for the selection of an optimal dwell time. Our analyses indicated that the optimum ratio of τ to dwell time is $\approx$50. This is greater than the ratio of 10 determined by Axelrod et al. (1976); however, the c.v.s of the fitted parameters did not increase substantially when the ratio of τ to dwell time was changed from 50 to 10. Thus, 10 is still a reasonable value to use as judged from our results. Despite the broad optimum for the ratio of τ to dwell time, the importance of optimizing the ratio of τ to dwell time is illustrated in Tables 5 and 6. The rapidity of our curve-fitting analysis for one-component diffusion and its accuracy make it superior to various linearization methods that have been proposed to estimate D values (Van Zoelen et al., 1983; Yguerabide et al., 1982). Significantly, the linearization methods are not capable of accurately determining diffusion parameters for a two-component model.

Analysis of two-component diffusion

The two-component curve-fitting analysis was able to accurately extract diffusion coefficients over a range of conditions. Analyses of simulated data demonstrated that the successful fit of a two-component model required a much greater signal level than for a one-component system. Optimization of beam power, beam diameter, dwell time, signal level, and depth of bleach are therefore more important if two-component analysis is required. Even with these optimizations, a high degree of confidence (c.v. < $\sim$0.2) in the fitted diffusion coefficients would require collection and analysis of multiple recovery curves to acquire a total of about 10,000 prebleach counts per channel (Table 8). As the ratio of the D values becomes larger (or smaller) than 10, the required signal level increases to achieve a given c.v. for both of the D values combined with reliable detection of the presence of two components (from Table 10).

For simulated data at lower signal levels, the error surface for the two-component fit sometimes has more than one minimum in the vicinity of the true parameter values as indicated by the observation that slightly different results are obtained when different starting guesses of the parameters are used. When the starting guesses for the weighted mobile fractions have the slow component more heavily weighted (starting $\alpha = 0.7$), the D values tended to be higher than the true values for the lower signal levels. With the fast component more heavily weighted (starting $\alpha = 0.3$), the D values had a tendency to be lower than the true values, were in general closer to the true values, and had significantly smaller c.v.s than when the slow component was more heavily weighted. Altering the α values did not change the conclusions drawn from the simulations except as noted above. In all of the results presented in this report, 0.3 was used for the starting guess for α. It is not clear in the cases in which there are at least two local minima near the true parameter values whether there is also a global minimum at

the true parameter values because the fitting algorithm used stops at the first minimum it finds.

Distinguishing one- and two-component recovery curves

Each recovery curve was fit to both one- and two-component models. If an F-test showed that the two-component fit had a significantly lower χ^2 value than the one-component fit, the recovery curve was considered two-component; otherwise, the recovery curve was considered a one-component one. One-component simulated data were identified readily by this test even at low signal levels (100 prebleach counts per channel; Table 3). Two-component simulated data required 1000 prebleach counts per channel as well as an optimized dwell time to achieve a similar degree of confidence in identification (Table 8). If the depth of bleach is increased to 0.9, then the same level of confidence is achieved at 316 prebleach counts per channel (Table 9). As the ratio of the D values of the two components decreases, the required signal level increases to achieve a given level of confidence in identifying two-component recoveries (from Table 10). Because signal level is often limiting in biological specimens and accurate measurements may require analysis of multiple recovery curves, one promising approach for analysis of multiple FRAP curves would be to use global analysis. This would allow the presumed constant values, such as the diffusion coefficients, to be determined from all of the recovery curves in concert, but would also allow determination of the values of individual variables such as the depth of bleach or mobile fraction for each individual recovery curve (Beechem, 1991).

In measurements of DiI diffusion in homogenous, liquid-crystalline liposomes, more than 81% of the cases were identified as one-component diffusion, irrespective of the objective lenses (beam diameters) or the dwell times used. However, when DiI diffusion was examined in the fibroblast plasma membrane, one-component diffusion was identified in 60% (19/32) of the cases and when rhodamine PE was used as the lipid probe, one-component diffusion was favored in 56% (35/63) of the cases. If one assumes that lipid diffusion in cell membranes should exhibit only one component, these results would suggest that our method could not distinguish reliably one- and two-component diffusion in cell plasma membranes. However, lipid diffusion in cell membranes may be more complicated than that which exists in the one-component simulations and homogeneous lipid vesicles. For example, the existence of lipid domains (Sheetz, 1993), transient binding of the diffusing molecule to immobile membrane components (Jacobson et al., 1987), or percolation of the diffusing molecule through a membrane of liquid and gel state domains (Almeida et al., 1992) may result in multicomponent lipid diffusion kinetics or long tailed diffusion kinetics (Nagle, 1992). Wolf and Voglmayr (1984) have documented that different regions of the sperm plasma membrane exhibit different lipid diffusional mobilities, and within cell membranes domains that differ in their phase (gel or fluid) (Klausner and Wolf, 1980; Wolf, 1988), have been identified. Other membrane probes, for example, the carbocyanine dyes, selectively partition into coexisting lipid membrane domains depending on their chain length relative to the chain length of the membrane lipids. It is possible that one or more of these situations exists in the fibroblast plasma membrane, resulting in the apparent ambiguity in choosing one- versus two-component diffusion despite the presence of a single-diffusing lipid indicator (e.g., Rhodamine PE or DiI). We have previously obtained data using fluorescence-quenching imaging, fluorescence resonance energy transfer, and digitized video fluorescence polarization microscopy (Wang et al., 1993; Florine-Casteel et al., 1991) that document the existence of lipid domains in the plasma membrane of living cells. Thus, the weight of the evidence suggests that lipid domains exist in the plasma membrane of living cells and account for the finding of both one- and two-component diffusion.

Optimization of FRAP data acquisition

To obtain the highest probability of selecting the proper model and accuracy of the curve fit, especially with respect to two-component data, it is necessary to optimize the conditions of data acquisition. Following is a brief simplified summary of steps to optimize FRAP data collection.

1) Maximize the beam diameter within the constraints of the experiment. We have not simulated the effects of finite pool size of the diffusing marker (cf. Elson and Qian, 1989); however, a crude guideline would be to make the fraction of the membrane surface covered by the irradiated spot as large as the expected c.v.s of the weighted mobile fraction parameters.
2) Choose the dwell time to optimize the ratio of τ to dwell time. Assuming that maximum monitoring beam power will be used, the dwell time should be chosen to be $\tau_2/52.3$ (optimal for the fast component) for a two-component recovery and $\tau/52.3$ for a one-component recovery.
3) Maximize the monitoring beam power constrained by the need to keep the bleaching due to monitoring negligible. One choice for the maximum is the largest beam power that does not produce detectable bleaching in a dry run experiment in which the bleach beam is not used.
4) Maximize the bleach beam power without damaging the specimen: there should be no change in appearance or in biologic or diffusional behavior of the specimen due to the bleach.

Comparison to other curve-fitting methods

The least-squared error method used in our studies is not a true maximum likelihood method for FRAP data at low signal levels, because the photon-counting noise is Poisson-distributed rather than Gaussian-distributed. Therefore, we tried using a true maximum likelihood method with the Marquardt algorithm for curve fitting, but there was no improvement in the results. We also tried using the modified

Gauss-Newton algorithm described by Johnson and Faunt (1992) with both the least-squared error method and the true maximum likelihood method but, again, there was no improvement in the results.

The method of Greenberg and Axelrod (1993) is the only other published method that measures D values for two diffusing components. This method uses the first two terms of the series solution and apparently a nonlinear curve fit algorithm as in the present method (although this was not explicitly stated in their manuscript). The present work differs from that of Greenberg and Axelrod in the following ways. 1) The present method uses several terms of the series solution to give greater precision, particularly when deeper bleaches are used. The results presented in this study show deeper bleaches to be critical in optimizing the data for analyzing two diffusing components. 2) Measurement errors in the present work were evaluated by the Monte Carlo method, which is more accurate for nonlinear curve fitting than the use of asymptotic SEs (Straume et al., 1991) used by Greenberg and Axelrod (1993). 4) The present work evaluates the performance of the curve fit analysis of FRAP data with regard to extraction of diffusion parameters and the determination of the number of diffusing components for a wide variety of specimens under a wide variety of instrumental conditions. These performance results appear to be broadly applicable to the method of Greenberg and Axelrod (1993), especially for shallow bleaches.

Thus, the algorithms described in this study permit the very accurate analysis of one-component diffusion and the ability to extract two-component diffusional parameters from biological membranes. The use of the models described in this study requires optimization of the acquisition of recovery curves and the availability of a statistical sample of FRAP recovery curves to choose between one- and two-component diffusion models in the absence of any other information about the system being studied.

We thank Dr. K. A. Jacobson for critical reading of the manuscript. We are grateful to Dr. Jacobson and Mr. Bing Yang for providing cells and probes for the membrane experiments. We thank Dr. C. R. Hackenbrock for his support.

This work was supported by grant AGO7218 from National Institutes of Health, the Gustavus and Louise Pfeiffer Research Foundation, and grant 88-16611 from the National Science Foundation.

REFERENCES

Almeida, P. F. F., W. L. C. Vaz, and T. E. Thompson. 1992. Lateral diffusion and percolation in two-phase, two-component lipid bilayers, topology of the solid-phase domains in-plane and across the lipid bilayer. *Biochemistry.* 31:7198–7210.

Axelrod, D., D. E. Koppel, J. Schlessinger, E. Elson, and W. W. Webb. 1976. Mobility measurement by analysis of fluorescence photobleaching recovery. *Biophys. J.* 16:1055–1069.

Barisas, G., and M. D. Leuther. 1979. Fluorescence photobleaching recovery measurement of protein absolute diffusion coefficients. *Biophys. Chem.* 10:221–229.

Beechem, J. M., E. Gratton, M. Ameloot, J. R. Knutson, and L. Brand. 1991. The global analysis of fluorescence intensity and anisotropy decay data: second-generation theory and programs. *In* Topics in Fluorescence Spectroscopy, Vol. 2. J. Lakowicz, editor. Plenum Press, New York. 241–306.

Bevington, P. R. 1969. Data Reduction and Error Analysis for the Physical Sciences. McGraw-Hill, New York. 336 pp.

Chazotte, B., and C. R. Hackenbrock. 1988. The multicollisional, obstructed, long-range diffusional nature of mitochondrial electron transport. *J. Biol. Chem.* 263:14359–14367.

Chazotte, B., E.-S. Wu, M. Hoechli, and C. R. Hackenbrock. 1985. Calcium-mediated fusion to produce ultra large osmotically active mitochondrial inner membranes of controlled protein density. *Biochim. Biophys. Acta.* 818:87–95.

Elson, E. L. 1985. Fluorescence correlation spectroscopy and photobleaching recovery. *Annu. Rev. Phys. Chem.* 36:379–406.

Elson, E. L., and H. Qian. 1989. Interpretation of fluorescence correlation spectroscopy and photobleaching recovery in terms of molecular interactions. *In* Methods in Cell Biology, Vol. 30. D. L. Taylor and Y.-L. Wang, editors. Academic Press, New York. 307–332.

Florine-Casteel, K. 1990. Phospholipid order in gel- and fluid-phase cell-size liposomes measured by digitized video fluorescence polarization microscopy. *Biophys. J.* 57:1199–1215.

Florine-Casteel, K., J. J. Lemasters, and B. Herman. 1991. Lipid order in hepatocyte plasma membrane blebs during ATP depletion measured by digitized video fluorescence polarization microscopy. *FASEB J.* 5:2078–2084.

Greenberg, M. L., and D. Axelrod. 1993. Anomalously slow mobility of fluorescent lipid probes in the plasma membrane of the yeast. *J. Membr. Biol.* 131:115–127.

Hoel, P. G., S. C. Port, and C. J. Stone. 1971. Introduction to Statistical Theory. Houghton Mifflin, Boston, MA. 237 pp.

Jacobson, K., A. Ishihara, and R. Inman. 1987. Lateral diffusion of proteins in membranes. *Annu. Rev. Physiol.* 49:163–175.

Jacobson, K., D. O'Dell, and T. J. August. 1984. Lateral diffusion of an 80,000-dalton glycoprotein in the plasma membrane of murine fibroblasts: relationships to cell structure and function. *J. Cell Biol.* 99:1624–1633.

James, D. R., and W. R. Ware. 1985. A fallacy in the interpretation of fluorescence decay parameters. *Chem. Phys. Lett.* 120:460–465.

Johnson, M. L., and L. M. Faunt. 1992. Parameter estimation by least squares methods. *Methods Enzymol.* 210:1–37.

Klausner, R. D., and D. E. Wolf. 1980. Selectivity of fluorescent lipid analogues for lipid domains. *Biochemistry.* 19:6199–6023.

Kapitza, H.-G., and K. A. Jacobson. 1986. Lateral motion of membrane proteins. *In* Techniques for the Analysis of Membrane Proteins. C. I. Ragan and R. J. Cherry, editors. Chapman and Hall, London. 345–375.

Mueller, P., T. F. Cien, and B. Rudy. 1983. Formation and properties of cell-size lipid bilayer vesicles. *Biophys. J.* 44:375–381.

Nagle, J. F. 1992. Long tail kinetics in biophysics? *Biophys. J.* 63: 366–370.

Peters, R. 1986. Fluorescence microphotolysis to measure nucleocytoplasmic transport and intracellular mobility. *Biochim. Biophys. Acta.* 864: 305–359.

Petersen, N. O., S. Felder, and E. L. Elson. 1986. Measurement of lateral diffusion by fluorescence photobleaching recovery. *In* Handbook of Experimental Immunology. D. M. Weir, editor. Blackwell Scientific Publishers, New York.

Press, W. H., B. P. Flannery, S. A. Teukolsky, and W. T. Vetterling. 1988. Numerical Recipes in C. Cambridge University Press, Cambridge. 735 pp.

Soumpasis, D. M. 1983. Theoretical analysis of fluorescence photobleaching recovery experiments. *Biophys, J.* 41:95–97.

Sheetz, M. P. 1993. Glycoprotein motility and dynamic domains in fluid plasma membranes. *Annu. Rev. Biophys. Biomol. Struct.* 22:417–431.

Straume, M., S. G. Frasier-Cadoret, and M. L. Johnson. 1991. Least-squares analysis of fluorescence data. *In* Topics in Fluorescence Spectroscopy, Vol. 2. J. Lakowicz, editor. Plenum Press, New York. 117–240.

Vaz, W. L. C., E. C. C. Melo, and T. E. Thompson. 1989. Translational diffusion and fluid domain connectivity in a two-component, two-phase phospholipid bilayer. *Biophys. J.* 56:869–876.

van Zoelen, E. J. J., G. J. Tertoolen, and S. W. de Laat. 1983. Simple computer method for evaluation of lateral diffusion coefficients from fluorescence photobleaching recovery kinetics. *Biophys. J.* 42:103–108.

Wang, X. F., J. J. Lemasters, and B. Herman. 1993. Plasma membrane architecture during hypoxic injury in rat hepatocytes measured by fluorescence quenching and resonance energy transfer imaging. *Bioimaging*. 1:30–39.

Wolf, D. E. 1988. Probing the lateral organization and dynamics of membranes. *In* Spectroscopic Membrane Probes, Vol. 1. L. M. Loew, editor. CRC Press, Boca Raton, FL. 193–220.

Wolf, D. E. 1989. Designing, building, and using a fluorescence recovery after photobleaching instrument. *In* Methods in Cell Biology, Vol. 30. D. L. Taylor and Y.-L. Wang, editors. Academic Press, New York. 271–306.

Wolf, D. E., and J. K. Voglmayr. 1984. Diffusion and regionalization in membranes of maturing ram sperm. *J. Cell Biol.* 98:1678–1684.

Yguerabide, J., J. A. Schmidt, and E. E. Yguerabide. 1982. Lateral mobility in membranes detected by fluorescence recovery after photobleaching. *Biophys. J.* 39:69–75.